

Microscopic Wave Functions of Spin Singlet and Nematic Mott States of Spin-One Bosons in High Dimensional Bipartite Lattices

Michiel Snoek and Fei Zhou

ITP, Utrecht University, Minnaert building, Leuvenlaan 4, 3584 CE Utrecht, The Netherlands

(Dated: May 22, 2019)

We present microscopic wave functions of spin singlet Mott insulating states and nematic Mott insulating states. We also investigate quantum phase transitions between the spin singlet Mott phase and the nematic Mott phase in both large- N limit and small- N limit (N being the number of particles per site) in high dimensional bipartite lattices. In the mean field approximation employed in this article we find that phase transitions are generally weakly first order.

PACS numbers: 03.75.Mn, 75.10.Jm, 75.45.+j, 05.30.Jp

I. INTRODUCTION

The recent observation of correlated states of bosonic atoms in optical lattices has generated much interest[1, 2]. As known for a while, when bosons in lattices interact with each other repulsively, they can be localized and form a Mott insulating state instead of a condensate[3, 4]. This phenomenon has been observed in the optical lattice experiment. By varying laser intensities of optical lattices, Greiner et al. have successfully investigated Mott states of spinless bosons by probing spin polarized cold atoms in optical lattices with a large potential depth[1, 2].

We are interested in spin correlated Mott insulating states of spin-one bosons, especially spin-one bosons with antiferromagnetic interactions. Some aspects of spin correlated Mott insulating states were investigated recently. For an even number of particles per site, both spin singlet Mott insulators and nematic Mott insulators were found in certain parameter regimes, while for high dimensional lattices with an odd number of particles per site only nematic insulating states were proposed [5]. In one-dimensional lattices, it was demonstrated that for an odd number of particles per site, Mott states should be dimerized valence-bond-crystals, which support interesting fractionalized quasi-excitations[6]. Effects of spin correlations on Mott insulator-superfluid transitions have been studied and remain to be fully understood[7].

In this article, we analyse the microscopic structures of spin singlet Mott insulating states (SSMI) and nematic Mott insulating states (NMI). We study, quantitatively, quantum phase transitions between these two phases in high-dimensional bipartite lattices. In the mean field approximation, we demonstrate that for an even number of particles per site, the transitions are weakly first order. The organisation is as follows. In section II, we present the general setting for the study of spin order-disorder quantum phase transitions. In section III, we present mean field results on the quantum phase transitions in both small N and large N limits. In section IV, we discuss issues which are to be understood in the future.

II. ALGEBRA AND SETTING

A. The microscopic Hamiltonian in the dilute limit

The microscopic lattice Hamiltonian we employ to study spin correlated states of spin-one bosons is:

$$\begin{aligned} \mathcal{H}_{\text{microscopic}} = & -t \sum_{\langle kl \rangle} (\psi_{k,m}^\dagger \psi_{l,m} + \text{h.c.}) \\ & + \sum_{k,l} \psi_{k,m}^\dagger \psi_{k,m} U^P(k,l) \psi_{l,m'}^\dagger \psi_{l,m'} \\ & + \sum_{k,l} \psi_{k,m}^\dagger S_{mn}^\gamma \psi_{kn} U^S(k,l) \psi_{l,m'}^\dagger S_{m'n'}^\gamma \psi_{l,n'} \end{aligned} \quad (1)$$

Here $\psi_{k,m}^\dagger$ is the creation operator of a spin-one particle at site k with spin-index $m = 0, \pm 1$. $\langle kl \rangle$ indicates that the sum should be taken over nearest neighbours and S^γ ($\gamma = x, y, z$) are spin-one matrix operators given as:

$$S^x = \frac{1}{\sqrt{2}} \begin{pmatrix} 0 & 1 & 0 \\ 1 & 0 & 1 \\ 0 & 1 & 0 \end{pmatrix}, \quad S^y = \frac{1}{\sqrt{2}} \begin{pmatrix} 0 & -i & 0 \\ i & 0 & -i \\ 0 & i & 0 \end{pmatrix}, \quad S^z = \begin{pmatrix} 1 & 0 & 0 \\ 0 & 0 & 0 \\ 0 & 0 & -1 \end{pmatrix}.$$

$U^P(k,l)$ and $U^S(k,l)$ are, respectively, spin-independent and spin-dependent interaction parameters between two bosons at site k and l .

In the dilute limit, which is defined as a limit where $\bar{\rho}a^3 \ll 1$ (a is the scattering length and $\bar{\rho}$ the average density), atoms scatter in s -wave channels. For two spin-one atoms, the scattering takes place in the total spin $S = 0, 2$ channels, with scattering lengths $a_{0,2}$. Interactions between atoms can be approximated as spin-dependent contact interactions [8]. In the lattice model introduced here, calculations yield

$$U^P(k,l) = E_c \delta_{kl} \quad \text{and} \quad U^S(k,l) = E_s \delta_{kl}. \quad (2)$$

The parameters E_c and E_s are given by:

$$E_c = \frac{4\pi\hbar^2\bar{\rho}(2a_2 + a_0)}{3MN} \tilde{c}, \quad E_s = \frac{4\pi\hbar^2\bar{\rho}(a_2 - a_0)}{3MN} \tilde{c}, \quad (3)$$

where N is the average number of atoms per site, M is the mass of atoms and \tilde{c} is a constant.

B. Algebras

For the study of spin correlated states in lattices, it is rather convenient to introduce the following operators:

$$\psi_{k,x}^\dagger = \frac{1}{\sqrt{2}}(\psi_{k,-1}^\dagger - \psi_{k,1}^\dagger) \quad (4a)$$

$$\psi_{k,y}^\dagger = \frac{i}{\sqrt{2}}(\psi_{k,-1}^\dagger + \psi_{k,1}^\dagger) \quad (4b)$$

$$\psi_{k,z}^\dagger = \psi_{k,0}^\dagger \quad (4c)$$

where k again labels a lattice site. In this representation:

$$\psi_{k,m}^\dagger S_{mn}^\alpha \psi_{k,n} = \hat{\mathbf{S}}_k^\alpha \equiv -i\epsilon^{\alpha\beta\gamma} \psi_{k,\beta}^\dagger \psi_{k,\gamma} \quad (5)$$

$\alpha, \beta, \gamma \in \{x, y, z\}$. The density operator can be expressed in a usual way:

$$\hat{\rho}_k \equiv \psi_{k,\gamma}^\dagger \psi_{k,\gamma} \quad (6)$$

Consequently the Hamiltonian is given as:

$$\mathcal{H}_{\text{latt}} = -\tilde{t} \sum_{\langle kl \rangle} (\psi_{k,\alpha}^\dagger \psi_{l,\alpha} + \text{h.c.}) + \sum_k E_c \hat{\rho}_k^2 + E_s \hat{\mathbf{S}}_k^2 - \hat{\rho}_k \mu \quad (7)$$

where we have introduced the chemical potential μ ; $\hat{\mathbf{S}}_k^2$ is the total spin operator $\hat{\mathbf{S}}_{k,\alpha} \hat{\mathbf{S}}_{k,\alpha}$.

$\psi_{k,\alpha}$ ($\alpha = x, y, z$) are bosonic operators obeying the following commutation relations:

$$[\psi_{k,\alpha}, \psi_{l,\beta}] = [\psi_{k,\alpha}^\dagger, \psi_{l,\beta}^\dagger] = 0, \quad [\psi_{k,\alpha}, \psi_{l,\beta}^\dagger] = \delta_{kl} \delta_{\alpha\beta}. \quad (8)$$

Taking into account Eqs. 5,6,8, one can verify the following algebras:

$$[\hat{\mathbf{S}}_k^\alpha, \psi_{l,\beta}] = \delta_{kl} i \epsilon^{\alpha\beta\gamma} \psi_{k,\gamma} \quad (9a)$$

$$[\hat{\mathbf{S}}_k^\alpha, \psi_{l,\beta}^\dagger] = \delta_{kl} i \epsilon^{\alpha\beta\gamma} \psi_{k,\gamma}^\dagger \quad (9b)$$

$$[\hat{\mathbf{S}}_k^\alpha, \hat{\mathbf{S}}_l^\beta] = \delta_{kl} i \epsilon^{\alpha\beta\gamma} \hat{\mathbf{S}}_k^\gamma \quad (9c)$$

$$[\hat{\rho}_k, \psi_{l,\alpha}] = -\delta_{kl} \psi_{k,\alpha} \quad (9d)$$

$$[\hat{\rho}_k, \psi_{l,\alpha}^\dagger] = \delta_{kl} \psi_{k,\alpha}^\dagger \quad (9e)$$

$$[\hat{\mathbf{S}}_k^\alpha, \hat{\rho}_l] = 0 \quad (9f)$$

Of particular interest is the singlet creation operator

$$\frac{1}{\sqrt{6}} \psi_{k,\alpha}^\dagger \psi_{k,\alpha}^\dagger = \frac{1}{\sqrt{6}} (\psi_{k,0}^\dagger \psi_{k,0}^\dagger - 2\psi_{k,1}^\dagger \psi_{k,-1}^\dagger). \quad (10)$$

We find the following properties for this operator:

$$[\hat{\mathbf{S}}_k^\alpha, \psi_{l,\alpha}^\dagger \psi_{l,\alpha}^\dagger] = [\hat{\mathbf{S}}_k^\alpha, \psi_{l,\alpha} \psi_{l,\alpha}] = 0; \quad (11a)$$

$$[\psi_{k,\alpha} \psi_{k,\alpha}, \psi_{l,\beta}^\dagger] = 2\delta_{kl} \psi_{k,\beta}; \quad (11b)$$

$$[\psi_{k,\alpha} \psi_{k,\alpha}, \psi_{l,\beta}^\dagger \psi_{l,\beta}^\dagger] = \delta_{kl} (4\hat{\rho}_k + 6). \quad (11c)$$

C. The on-site dynamics

The total spin operator can be expressed as:

$$\hat{\mathbf{S}}_k^2 = \hat{\rho}_k (\hat{\rho}_k + 1) - \psi_{k,\alpha}^\dagger \psi_{k,\alpha}^\dagger \psi_{k,\beta} \psi_{k,\beta}. \quad (12)$$

So, eigenstates of the total spin operator have to be eigenstates of the "singlet counting operator" $\psi_{k,\alpha}^\dagger \psi_{k,\alpha}^\dagger \psi_{k,\beta} \psi_{k,\beta}$.

Defining the state $\Psi_{k,0}^n$ such that:

$$\hat{\rho}_k \Psi_{k,0}^n = n \Psi_{k,0}^n, \quad \psi_{k,\alpha}^\dagger \psi_{k,\alpha}^\dagger \psi_{k,\beta} \psi_{k,\beta} \Psi_{k,0}^n = 0, \quad (13)$$

we find that wave functions of these eigenstates are:

$$\Psi_{k,m}^n = C (\psi_{k,\alpha}^\dagger \psi_{k,\alpha}^\dagger)^m \Psi_{k,0}^{n-2m} \quad (14)$$

where C is a normalization constant. From Eq. (11c) it follows that:

$$\psi_{k,\alpha}^\dagger \psi_{k,\alpha}^\dagger \psi_{k,\beta} \psi_{k,\beta} \Psi_{k,m}^n = (4m(n-m) + 2m) \Psi_{k,m}^n \quad (15)$$

Using that $\hat{\rho}_k \Psi_{k,m}^n = n \Psi_{k,m}^n$ we derive:

$$\hat{\mathbf{S}}_k^2 \Psi_{k,m}^n = (n-2m)(n-2m+1) \Psi_{k,m}^n. \quad (16)$$

So $S_k = n - 2m$. Now if n is even, S_k is also even and when n is odd, S_k is odd too. For an even number of particles per site N the excitations labelled by $S_k = 0, 2, 4, \dots, N$ are present, whereas for an odd number of particles per site $S_k = 1, 3, 5, \dots, N$ are allowed. This reflects the basic property of the many body wave function of spin-one bosons, which has to be symmetric under the interchange of two particles.

Solutions for spin correlated condensates with finite numbers of particles were previously obtained[9]; in the thermodynamical limit, these states evolve into polar condensates [8, 10, 11]. Also there, two-body scatterings were shown to lead to either "antiferromagnetic" or "ferromagnetic" spin correlations in condensates. Spin correlated condensates have been investigated in experiments [12, 13].

D. The effective Hamiltonian for Mott states

In the limit when $t \ll E_c$, atoms are localized and only virtual exchange processes are allowed. An effective Hamiltonian in this limit can be derived in a second order perturbative calculation of the Hamiltonian in Eq. 7:

$$\mathcal{H}_{\text{Mott}} = \sum_k \frac{\hat{\mathbf{S}}_k^2}{2I} - J_{\text{ex}} \sum_{\langle kl \rangle} \left(\psi_{k,\alpha}^\dagger \psi_{l,\alpha} \psi_{l,\beta}^\dagger \psi_{k,\beta} + \text{h.c.} \right). \quad (17)$$

Here $J_{\text{ex}} = \frac{\tilde{t}^2}{2E_c}$. In deriving Eq. 17, we have taken into account that $E_s \ll E_c$.

To facilitate discussions, we introduce the following operator:

$$\hat{Q}_{k,\alpha\beta} = \psi_{k,\alpha}^\dagger \psi_{k,\beta} - \frac{1}{3} \delta_{\alpha\beta} \psi_{k,\gamma}^\dagger \psi_{k,\gamma}, \quad (18)$$

whose expectation value

$$\tilde{Q} = \frac{\langle \hat{Q}_{\alpha\beta} \rangle}{\langle \hat{Q}_{\alpha\beta} \rangle_{\text{ref}}} \quad (19)$$

is the nematic order parameter. The reference state $\psi_{\text{ref}} = \frac{(\mathbf{n}_\alpha \psi_\alpha)^N}{\sqrt{N!}} |\text{vac}\rangle$ is a maximally ordered state. Choosing $\mathbf{n} = \mathbf{e}_z$, we obtain:

$$\langle \hat{Q}_{\alpha\beta} \rangle_{\text{ref}} = N \begin{pmatrix} -\frac{1}{3} & 0 & 0 \\ 0 & -\frac{1}{3} & 0 \\ 0 & 0 & \frac{2}{3} \end{pmatrix}. \quad (20)$$

\tilde{Q} varies in a range of $[-\frac{1}{2}, 1]$.

In terms of the operator $\hat{Q}_{\alpha\beta}$, the effective Mott Hamiltonian can be rewritten as (up to an energy shift):

$$\mathcal{H}_{\text{eff}} = E_s \sum_k \text{Tr}[\hat{Q}_k \hat{Q}_k - \hat{Q}_k \hat{Q}_k^\dagger] - J_{\text{ex}} \sum_{\langle kl \rangle} \text{Tr}[\hat{Q}_k \hat{Q}_l] \quad (21)$$

Finally we define

$$\eta = \frac{z J_{\text{ex}}}{E_s} \quad (22)$$

as a dimensionless parameter, which can be varied continuously; z is the coordination number of the lattice.

E. The range of the physical parameters

From Eq. 3 it is clear that E_s and E_c depend on the density, number of atoms, the mass of atoms and scattering lengths. However, their ratio depends only on the scattering lengths. According to current estimates [14, 15], for sodium atoms this ratio is given as $\frac{E_s}{E_c} \approx 9 \cdot 10^{-2}$. In this paper, we are interested in the limit $E_s \ll E_c$.

The parameter \tilde{t} can be varied independently by changing the depth of the optical lattice. A wide range is experimentally accessible; one can vary from the regime where $\tilde{t} \gg E_c$ to a regime where $\tilde{t} \ll E_s$. We limit ourselves to Mott states ($\tilde{t} \ll E_c$), where all bosons are localized, but the ratio η can have arbitrary values.

III. PHASE TRANSITIONS BETWEEN SSMI'S AND NMI'S

A. Two particles per site

In the case of two particles per site, the on-site Hilbert space is six-dimensional, including a spin singlet state

$$|S = 0, S_z = 0\rangle = \frac{\psi_\eta^\dagger \psi_\eta^\dagger}{\sqrt{6}} |0\rangle, \quad (23)$$

and five spin $S = 2$ -states

$$|Q_{\eta\xi}\rangle = \frac{\sqrt{3}}{2} Q_{\eta\xi} \psi_\eta^\dagger \psi_\xi^\dagger |0\rangle \quad (24)$$

where $Q_{\eta\xi}$ is a symmetric and traceless tensor with five independent elements. All states in the Hilbert space are symmetric under the interchange of bosons; as expected, the states $|Q_{\eta\xi}\rangle$ are orthogonal to $|S = 0, S_z = 0\rangle$. It is convenient to choose the following representation of $Q_{\eta\xi}$:

$$Q_{\eta\xi}(\mathbf{n}) = \mathbf{n}_\eta \mathbf{n}_\xi - \frac{1}{3} \delta_{\eta\xi}, \quad (25)$$

with the director \mathbf{n} as a unit vector living on S^2 . States defined by the director \mathbf{n} form an over-complete set in the subspace spanned by five $S = 2$ states.

When the hopping is zero, one notices that the Hamiltonian in Eq.17 commutes with $\hat{\mathbf{S}}_k^2$; the ground state wave function is

$$|\Psi\rangle = \prod_k |S = 0, S_z = 0\rangle_k. \quad (26)$$

On the other hand, when E_s goes to zero, the Hamiltonian commutes with $\text{Tr}[\hat{Q}_{k,\alpha\beta} \hat{Q}_{l,\beta\alpha}]$ and the ground state wave function can be confirmed as:

$$|\Psi\rangle = \prod_k \sqrt{\frac{2}{3}} |Q(\mathbf{n})\rangle_k + \frac{1}{\sqrt{3}} |S = 0, S_z = 0\rangle_k. \quad (27)$$

for any choice of the director \mathbf{n} .

To study spin nematic or spin singlet Mott states at an arbitrary η , we introduce a trial wave function which is a linear superposition of singlet states and symmetry breaking states:

$$|\Psi\rangle_\theta = \prod_k \cos \theta |S = 0, S_z = 0\rangle_k + \sin \theta |Q_{\eta\xi}(\mathbf{n})\rangle_k. \quad (28)$$

Here θ is a variable to be determined by the variational method.

A straightforward calculation leads to the following results:

$$E(\theta) = \langle \Psi | \mathcal{H} | \Psi \rangle_\theta \quad (29)$$

$$= 6E_s \sin^2 \theta - z J_{\text{ex}} \frac{2}{3} ((2\sqrt{2} \cos \theta \sin \theta + \sin^2 \theta)^2$$

$$\tilde{Q} = (\sqrt{2} \cos \theta \sin \theta + \frac{\sin^2 \theta}{2}) \quad (30)$$

In terms of \tilde{Q} , the energy can be expressed as:

$$E = 6E_s \left(\frac{4}{9} + \frac{2}{9} \tilde{Q} - \frac{4}{9} \sqrt{-2\tilde{Q}^2 + \tilde{Q} + 1} \right) - \frac{8}{3} z J_{\text{ex}} \tilde{Q}^2,$$

which for $\tilde{Q} \ll 1$ can be expanded as:

$$\left(3E_s - \frac{8}{3} z J_{\text{ex}} \right) \tilde{Q}^2 - \frac{3}{2} E_s \tilde{Q}^3 + \frac{39}{16} E_s \tilde{Q}^4 + \dots \quad (31)$$

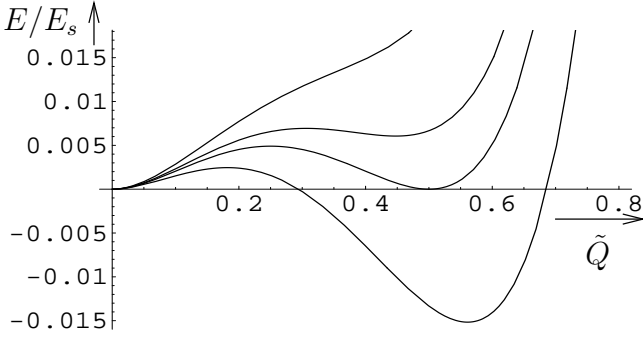


FIG. 1: Energy (measured in units of E_s) versus \tilde{Q} for various η for $N = 2$. Curves from top to bottom are for $\eta = 0.97, 0.99, 1.0, 1.02$.

The cubic term leads to a first order phase transition in the mean field approximation, which is similar to the situation in classical nematic liquid crystals [17].

In FIG.1 the \tilde{Q} -dependence of the energy is plotted for various η in the vicinity of a quantum critical point (mean field). For $\eta < 0.985$, the energy has only one minimum at $\tilde{Q} = 0$ and correspondingly the ground state is a spin singlet Mott state. When $0.985 < \eta < 1.0$, in addition to the global minimum at $\tilde{Q} = 0$, there appears a local minimum at $\tilde{Q} > 0$, which represents a spin nematic metastable state. When $\eta > 1.0$ the solution with $\tilde{Q} > 0$ becomes a global minimum and the solution at $\tilde{Q} = 0$ is metastable; consequently the ground state is a nematic Mott state. For $\eta > \frac{9}{8}$, the solution at $\tilde{Q} = 0$ becomes unstable ; but an additional local minimum appears at $\tilde{Q} < 0$ which we interpret as a new metastable state (not shown in FIG. 1).

The evolution of ground states as η is varied, is summarized in FIG. 2. As is clearly visible, the phase transition is a weakly first order one. The jump in \tilde{Q} at the phase-transition ($\eta = 1.0$) is equal to $\frac{1}{2}$.

It is worth emphasising that a positive \tilde{Q} corresponds to a rod-like nematic state; for $\tilde{Q} = 1$ the state is microscopically given by:

$$\frac{(\mathbf{n}_\alpha \psi_\alpha^\dagger)^2}{\sqrt{2}} |0\rangle. \quad (32)$$

A solution with negative \tilde{Q} indicates a disk-like nematic state; the microscopic wave function is

$$\left(\frac{1}{2} \psi_\eta^\dagger \psi_\eta^\dagger - \frac{(\mathbf{n}_\alpha \psi_\alpha^\dagger)^2}{2} \right) |0\rangle. \quad (33)$$

at $\tilde{Q} = -\frac{1}{2}$. For $\mathbf{n} = \mathbf{e}_z$ the wave functions are $\frac{1}{\sqrt{2}} \psi_z^\dagger \psi_z^\dagger |0\rangle$ and $\frac{1}{2} (\psi_x^\dagger \psi_x^\dagger + \psi_y^\dagger \psi_y^\dagger) |0\rangle$ respectively.

We have also tried a five-parameter variational approach, taking into account the full on-site Hilbert space. In a slightly different representation we write the trial

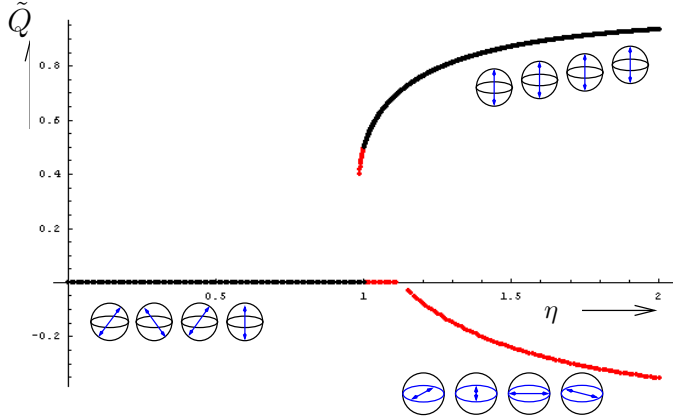


FIG. 2: The nematic order parameter as a function of η for $N = 2$. The phase transition takes place at $\eta = 1$. Data along the black line represent ground states; the red line is for metastable states. Spheres with double-headed arrows are introduced to represent ordering in director \mathbf{n} defined in Eq. 25 in different Mott states. In spin singlet states, the director \mathbf{n} is uncorrelated; in rod-like nematic states, the director \mathbf{n} is ordered and in disk-like states, the axis of the easy plane of the director \mathbf{n} is ordered.

wave function as:

$$|\Psi\rangle = \prod_k (c_{xx}|xx\rangle_k + c_{yy}|yy\rangle_k + c_{zz}|zz\rangle_k + c_{xy}|xy\rangle_k + c_{xz}|xz\rangle_k + c_{yz}|yz\rangle_k) \quad (34)$$

Here $|\alpha\alpha\rangle_k = \frac{1}{\sqrt{2}} \psi_{k,\alpha}^\dagger \psi_{k,\alpha}^\dagger |0\rangle$ (no summation) and $|\alpha\beta\rangle_k = \psi_{k,\alpha}^\dagger \psi_{k,\beta}^\dagger |0\rangle$. This results in the following expression for the energy:

$$\begin{aligned} E = & E_s [4(c_{xx}^2 + c_{yy}^2 + c_{zz}^2 - c_{xx}c_{yy} - c_{xx}c_{zz} - c_{yy}c_{zz}) \\ & + 6(c_{xy}^2 + c_{xz}^2 + c_{yz}^2)] \\ & - zJ_{\text{ex}} [6(c_{xx}^4 + c_{yy}^4 + c_{zz}^4) + 4(c_{xy}^4 + c_{xz}^4 + c_{yz}^4) \\ & + 4(c_{xx}^2 c_{yy}^2 + c_{xx}^2 c_{zz}^2 + c_{yy}^2 c_{zz}^2) \\ & + 12(c_{xx}^2 c_{xy}^2 + c_{xx}^2 c_{xz}^2 + c_{yy}^2 c_{xy}^2 + c_{yy}^2 c_{yz}^2 \\ & + c_{zz}^2 c_{xz}^2 + c_{zz}^2 c_{yz}^2) \\ & + 8(c_{xy}^2 c_{xz}^2 + c_{xy}^2 c_{yz}^2 + c_{xz}^2 c_{yz}^2) \\ & + 8\sqrt{2}(c_{xx} + c_{yy} + c_{zz}) c_{xy} c_{xz} c_{yz} \\ & + 4(c_{xx}^2 c_{yz}^2 + c_{yy}^2 c_{xz}^2 + c_{zz}^2 c_{xy}^2) \\ & + 8(c_{xx} c_{yy} c_{xy}^2 + c_{xx} c_{zz} c_{xz}^2 + c_{yy} c_{zz} c_{xz}^2)]. \end{aligned} \quad (35)$$

The conclusions are almost the same and summarized below:

- For $\eta < 0.985$. the only minimum is at $c_{xx} = c_{yy} = c_{zz} = \frac{1}{\sqrt{3}}$, $c_{\alpha\beta} = 0$ for $\alpha \neq \beta$.
- At $\eta = 0.985$ additional local minima appear.
- At $\eta = 1$ a first order phase transition takes place.

- iv) For $\frac{8}{9} > \eta > 1$, the global minimum is at $\tilde{Q} > 0$, but the $\tilde{Q} = 0$ -solution remains to be a local minimum.
- v) At $\eta = \frac{9}{8}$ the solution at $c_{xx} = c_{yy} = c_{zz} = \frac{1}{\sqrt{3}}$ becomes unstable.
- vi) However, the disk-like $\tilde{Q} < 0$ -solution appears in this case as a saddle point.

B. An even number of particles per site

For a large number of particles per site, it is convenient to introduce the following coherent state representation:

$$|\mathbf{n}, \chi\rangle = \frac{1}{\sqrt{2\delta N}} \sum_{m=N-\delta N}^{N+\delta N} \exp(-im\chi) \frac{(\mathbf{n}_\alpha)^m \psi_\alpha^\dagger}{\sqrt{2(m-1)!}} \quad (36)$$

where the director \mathbf{n} is again a unit vector on S^2 given by $(\cos \phi \sin \theta, \sin \phi \sin \theta, \cos \theta)$. In this representation

$$\hat{\rho} = i \frac{\partial}{\partial \chi_k} \quad (37)$$

$$\hat{\mathbf{S}} = i \mathbf{n} \times \frac{\partial}{\partial \mathbf{n}} \quad (38)$$

$$\hat{\mathbf{S}}^2 = - \left[\frac{1}{\sin \theta} \frac{\partial}{\partial \theta} \left(\sin \theta \frac{\partial}{\partial \theta} \right) + \frac{1}{\sin^2 \theta} \frac{\partial^2}{\partial \phi^2} \right] \quad (39)$$

$$\hat{Q}_{\alpha\beta} = N \left(\mathbf{n}_\alpha \mathbf{n}_\beta - \frac{1}{3} \delta_{\alpha\beta} \right) \quad (40)$$

The Hamiltonian in Eq. 7 can be mapped to a Constrained Quantum Rotor Model (CQR), describing the dynamics of two unit vectors $(\mathbf{n}, e^{i\chi})$ on a two-sphere and a unit circle:

$$\mathcal{H}_{\text{CQR}} = -t \sum_{\langle kl \rangle} \mathbf{n}_k \cdot \mathbf{n}_l \cos(\chi_k - \chi_l) + \sum_k E_s \hat{\mathbf{S}}_k^2 + E_c \hat{\rho}_k^2 - \hat{\rho}_k \mu \quad (41)$$

$t = N\tilde{t}$. The CQR-model has been introduced to study spin-one bosons in a few previous works and we refer to those papers for detailed discussions [5, 6, 16]. For Mott states the effective Hamiltonian can be found as:

$$\mathcal{H} = E_s \sum_k \mathbf{S}_k^2 - J_{\text{ex}} \sum_{\langle kl \rangle} (\mathbf{n}_k \cdot \mathbf{n}_l)^2; \quad J_{\text{ex}} = \frac{t^2}{2E_c}, \quad (42)$$

In general, we choose the on-site trial wave function to be:

$$\psi(\mathbf{n}_k) = C_\sigma \exp \left[\frac{\sigma}{2} (\mathbf{n}_k \cdot \mathbf{n}_0)^2 \right]. \quad (43)$$

C_σ is a normalization constant. When $\sigma \rightarrow 0$ this yields an isotropic state $Y_{00}(\mathbf{n}_k)$, which indicates a spin singlet state. When $\sigma \rightarrow +\infty$, \mathbf{n}_k is localized on the two-sphere in the vicinity of \mathbf{n}_0 , representing a rod-like nematic state and when $\sigma \rightarrow -\infty$, \mathbf{n}_k lies in a plane perpendicular to \mathbf{n}_0 , corresponding to a disk-like spin nematic state. Moreover this wave function has the following property: $\psi(-\mathbf{n}_k) = \psi(\mathbf{n}_k)$ as is required for an even number of particles per site [16].

Choosing $\mathbf{n}_0 = e_z$ this gives:

$$\psi(\phi_k, \theta_k) = C_\sigma \exp \left[\frac{\sigma^2}{2} \cos^2 \theta_k \right] \quad (44)$$

The expectation value of the Hamiltonian in this state is:

$$E_\sigma = E_s \left(-\frac{3}{4} - \frac{1}{2} \sigma + \frac{3e^\sigma \sqrt{|\sigma|}}{2\sqrt{\pi} \text{Erfi} \sqrt{|\sigma|}} \right) - z J_{\text{ex}} \left(\frac{12e^{2\sigma} \sigma - 4e^\sigma \sqrt{\pi} \sqrt{|\sigma|} (3 + 2\sigma) \text{Erfi} \sqrt{|\sigma|} + \pi (3 + 4(\sigma + \sigma^2)) \text{Erfi}^2 \sqrt{|\sigma|}}{8\pi\sigma^2 \text{Erfi}^2 \sqrt{|\sigma|}} \right)$$

in which $\text{Erfi}[x]$ is the complex error function defined by $\text{Erf}[ix]/i$. In a series expansion for $\sigma \ll 1$, the result is:

$$-\frac{z J_{\text{ex}}}{3} + \left(\frac{2}{15} E_s - \frac{8}{675} z J_{\text{ex}} \right) \sigma^2 + \left(\frac{4}{315} E_s - \frac{32}{14175} z J_{\text{ex}} \right) \sigma^3 + \left(-\frac{8}{4725} E_s + \frac{32}{165375} z J_{\text{ex}} \right) \sigma^4 + o(\sigma^{10}) \quad (45)$$

The energy as a function of σ at different η is plotted in FIG. 3, which is qualitatively the same as FIG. 1 for two particles per site. When $\eta < 9.96$, the energy as a function of σ has only one (global) minimum, which corresponds to a spin singlet ground state. When

$\eta > 9.96$, in addition to the global minimum, there appears a local minimum at $\sigma > 0$. At $\eta = \eta_c = 10.0965$, these two minima become degenerate, signifying a phase transition. At $\eta > \eta_c$, the solution at $\sigma = 0$ becomes a local minimum indicating a metastable spin singlet state,

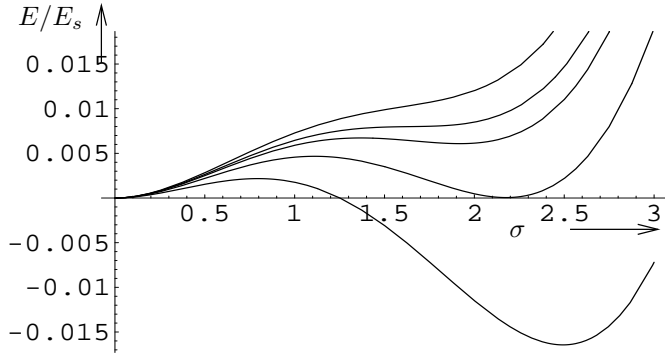


FIG. 3: Energy (in units of E_s) as a function of σ for various η ($N = 2k \gg 1$). From top to bottom are curves for $\eta = 9.9, 9.96, 10, 10.0965, 10.3$.

whereas the global minimum at $\sigma > 0$ corresponds to a nematic ground state. As η further increases, the solution at $\sigma = 0$ becomes unstable and a local minimum occurs at $\sigma < 0$, while the global minimum remains at $\sigma > 0$. Following discussions on Eqs. 32,33 we interpret the $\sigma < 0$ solution as a metastable disk-like spin nematics.

For the trial wave function in Eq. 45 the nematic order parameter can be calculated as:

$$\begin{aligned} \tilde{Q} &= \frac{\langle \sigma | \hat{Q}_{\alpha\beta} | \sigma \rangle}{\langle \infty | \hat{Q}_{\alpha\beta} | \infty \rangle} \\ &= -\frac{1}{2} - \frac{3}{4\sigma} + \frac{3e^\sigma}{2\sqrt{\pi|\sigma|} \operatorname{Erfi}\sqrt{|\sigma|}} \end{aligned} \quad (46)$$

When \tilde{Q} is small, we obtain an expression of the energy in terms of \tilde{Q} :

$$E_{\tilde{Q}} = -\frac{zJ_{\text{ex}}}{3} + \left(\frac{15}{2}E_s - \frac{2}{3}zJ_{\text{ex}} \right) \tilde{Q}^2 - \frac{75}{14}E_s \tilde{Q}^3 + \frac{1275}{98}E_s \tilde{Q}^4 \quad (47)$$

The jump in \tilde{Q} at the phase transition is equal to .323377.

The evolution of ground state wave functions and results on quantum phase transitions are summarized in figure 4, where the nematic order parameter is plotted as a function of η .

C. An odd number of particles per site

At last, we also present results for an odd number of atoms per site. The main difference between this case and the case for an even number of particles per site is that at zero hopping limit in the former case there is always an unpaired atom at each site. Consequently in the mean field approximation, we only find nematic Mott insulating phases. We expect this approximation

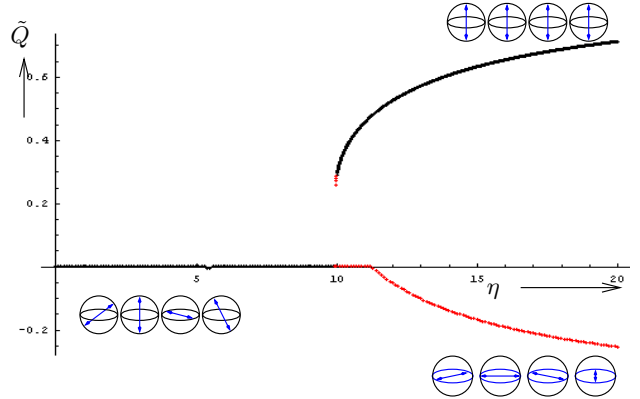


FIG. 4: Nematic order parameter as a function of η for $N = 2k (\gg 1)$. Along the black lines are ground states; along the red lines are metastable states. (See also the caption of FIG. 2.)

to be valid in high dimensional lattices but to fail in low dimensions, especially in one-dimensional lattices where long wave length fluctuations are substantial. Here we restrict ourselves to high dimensional lattices only.

For large N a trial wave function which interpolates between spin singlet states (dimerized) and nematic states can be introduced as:

$$\Psi_{\text{odd}}(\{\mathbf{n}_k\}) = \prod_{\langle kl \rangle_p} C(O, \sigma) (O(\mathbf{n}_k \cdot \mathbf{n}_0)(\mathbf{n}_l \cdot \mathbf{n}_0) + (\mathbf{n}_k \cdot \mathbf{n}_l)) \times \exp[\sigma((\mathbf{n}_k \cdot \mathbf{n}_0)^2 + (\mathbf{n}_l \cdot \mathbf{n}_0)^2)]. \quad (48)$$

$\langle kl \rangle_p$ denotes that the summation should be taken over parallelly ordered pairs of nearest neighbours k and l covering the lattice. $C(O, \sigma)$ is a normalization constant. The solution with $O = 0, \sigma = 0$ corresponds to a dimerized valence bond crystal state; and solutions with $O \neq 0$, or $\sigma \neq 0$ represent nematic states.

It is straightforward, but tedious to compute the energy of these states. Minimizing it for various values of η for $d = 3$ gives the results shown in FIG. 5 and 6. Up to $\eta = 1$ no phase transitions are found in the mean field approximation; and ground states break both rotational and translational symmetries [18].

At very small η , the on-site Hilbert space is truncated into the one for a spin-one particle[6]. The reduced Hamiltonian in the truncated space is a Bilinear-Biquadratic model for spin-1 lattices

$$\mathcal{H}_{b,b} = J \sum_{\langle kl \rangle} [\cos \theta \mathbf{S}_k \cdot \mathbf{S}_l + \sin \theta (\mathbf{S}_k \cdot \mathbf{S}_l)^2], \mathbf{S}_k^2 = 2; \quad (49)$$

θ in general varies between $-3\pi/4$ and $-\pi/2$. We therefore expect ground states at small η limit should still exhibit nematic order (i.e. $O \neq 0$).

It is worth emphasizing that conclusions about small η limit arrived here are only valid in high dimensional

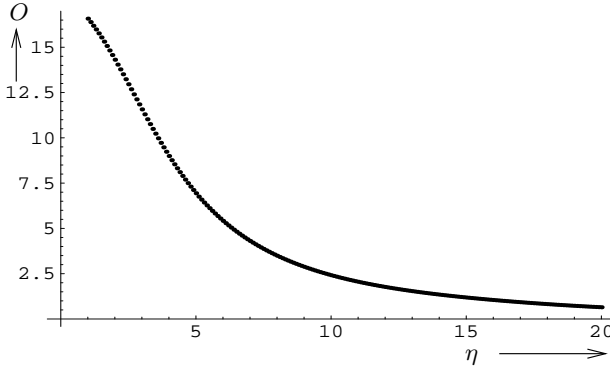


FIG. 5: The value of O as a function of η ($N = 2k + 1 \gg 1$).

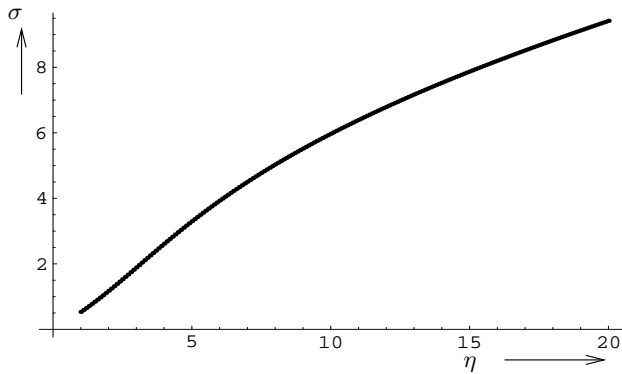


FIG. 6: The value of σ as a function of η ($N = 2k + 1 \gg 1$).

bipartite lattices. In low dimensional lattices, states of correlated atoms in this limit was discussed recently and ground states could be rotationally invariant dimerized-valence-bond crystals[6].

IV. CONCLUSIONS

We have studied the microscopic wave functions of spin nematic and spin singlet Mott states. Both disk-like and rod-like spin nematic states were investigated. We also have analysed quantum phase transitions between the spin singlet Mott insulating state and the nematic Mott insulating state. We show that in the mean field approximation, the phase transitions are weakly first order ones. Thus, we expect that fluctuations play a very important role in these transitions and the full theory on quantum phase transitions remains to be discovered.

On the other hand, we have estimated fluctuations in different regimes of the parameter space. We found that fluctuations are indeed small away from the critical point, at either small hopping or large hopping limit for an even number of particles per site. For the small hopping limit, fluctuations are proportional to η , while for large hopping limit they can be estimated as being proportional to $\frac{1}{\eta}$.

For an odd number of particles per site, fluctuations are small only at large hopping limit and are significant at small hopping limit. The later fact implies a large degeneracy of Mott states at zero hopping limit which was emphasised in the discussions on low dimensional Mott states. The physics in this limit remains to be fully understood.

In the context of antiferromagnets, spin nematic states have also been proposed [19, 20, 21]. Collective excitations in atomic nematic states should be similar to those studied in previous works and we refer to [19, 20, 21] for details.

V. ACKNOWLEDGEMENT

This work is supported by the foundation FOM, in the Netherlands under contract 00CCSPP10m 02SIC25 and NWO-MK projectruimte 00PR1929; MS is also partially supported by a grant from Utrecht University.

Note added: At a later stage of this work, we received a copy of the manuscript by A. Imambekov, M. Lukin and E. Demler where similar conclusions have been arrived.

APPENDIX A: AN ALTERNATIVE DESCRIPTION

Alternatively, one can also carry out the calculations in section III, using the following operator:

$$\begin{aligned} \hat{Q}_{2,\alpha\alpha'} &= \hat{\mathbf{S}}^\alpha \hat{\mathbf{S}}^{\alpha'} - \frac{1}{3} \delta_{\alpha\alpha'} \hat{\mathbf{S}}^\gamma \hat{\mathbf{S}}^\gamma \\ &= -\epsilon^{\alpha\beta\gamma} \epsilon^{\alpha'\beta'\gamma'} \psi_\beta^\dagger \psi_{\beta'}^\dagger \psi_\gamma \psi_{\gamma'} + \delta_{\alpha\alpha'} \psi_\eta^\dagger \psi_\eta \\ &\quad - \psi_{\alpha'}^\dagger \psi_\alpha - \frac{1}{3} \delta_{\alpha\alpha'} \hat{\mathbf{S}}_{\text{tot}}^2 \end{aligned} \quad (\text{A1})$$

Defining the more conventional order parameter [19]

$$\tilde{Q}_2 = \frac{\langle \hat{Q}_{2,\alpha\alpha'} \rangle}{\langle \hat{Q}_{2,\alpha\alpha'} \rangle_{\text{ref}}}, \quad (\text{A2})$$

we obtain the following results for the trial wavefunction in Eq. 28:

$$\begin{aligned}
\tilde{Q}_2 &= \sqrt{\frac{3}{2}} \sin^2 \theta \\
E &= 6E_s \sqrt{\frac{2}{3}} \tilde{Q}_2 \\
&\quad - \frac{2}{3} z J_{\text{ex}} \left(2\sqrt{2} \sqrt{\sqrt{\frac{2}{3}}(1 - \sqrt{\frac{2}{3}} \tilde{Q}_2) \tilde{Q}_2 + \sqrt{\frac{2}{3}} \tilde{Q}_2} \right)^2 \\
&= \left(2\sqrt{6} E_s - \frac{16}{3} \sqrt{\frac{2}{3}} z J_{\text{ex}} \right) \tilde{Q}_2 \\
&\quad - \frac{16\sqrt[4]{2}}{\sqrt[4]{3^7}} z J_{\text{ex}} \tilde{Q}_2^{3/2} + \frac{28}{9} z J_{\text{ex}} \tilde{Q}_2^2 + O(\tilde{Q}_2^{5/2})
\end{aligned}$$

which lead to the same conclusions as in section III. However, in terms of the order parameter defined in Eq. A2, the rod-like and disk-like structures shown in FIG.2 and FIG.4 are less obvious.

In the case of a large number of particle per site, the order parameter introduced here has the same expectation value as the operator in Eq. 40.

[1] M. Greiner et al., *Nature* **415**, 39 (2002).
[2] M. Greiner et al. *Nature* **419**, 51 (2002).
[3] M. P. A Fisher, P. B. Weichman, G. Grinstein and D.S. Fisher, *Phys. Rev. B* **40**, 546 (1989).
[4] D. Jaksch et al. *Phys. Rev. lett.* **81**, 3108 (1998).
[5] E. Demler and F. Zhou, *Phys. Rev. Lett.* **88**, 163001-1 (2002)
[6] F. Zhou, cond-mat/0207041; F. Zhou and M. Snoek, to appear (June, 2003).
[7] S. Tsuchiya and S. Kuhira, cond-mat/0209676
[8] T. L. Ho, *Phys. Rev. Lett.* **81**, 742 (1998).
[9] C.K. Law, H. Pu and N.P. Bigelow, *Phys. Rev. Lett.* **81**, 5257 (1998).
[10] T. Ohmi and K. Machinda, *Journal of the Physical Society of Japan* **76**, 1822 (1998).
[11] Y. Castin and C. Herzog, cond-mat/0012040
[12] D. Stamper-Kurn et al., *Phys. Rev. Lett.* **80**, 2027 (1998).
[13] J. Stenger et a., *Nature* **396**, 345 (1998).
[14] J. P. Burke Jr., C.H. Green and J.L. Bohn, *Phys. Rev. Lett.* **81**, 5257 (1998).
[15] C.V. Ciobanu, S. K. Yip and T. L. Ho, *Phys. Rev. A* **61**, 033607 (2002).
[16] Fei Zhou, *Phys. Rev. Lett.* **87**, 080401-1 (2001); cond-mat/0108473, to appear in *Int. Jour. of Mod. Phys. B*, (June, 2003).
[17] P.G. de Gennes, *The physics of liquid crystals*, Oxford University Press, 1974.
[18] At the time of submission, we noticed that nematic states for one particle per site were also addressed very recently in S.K. Yip, cond-mat/0306018. The 3D results there are consistent with the mean field results in Section III C. However, most one-dimensional states proposed in that paper break the rotational symmetry and are unlikely to be candidates for true ground states. Some general discussions on one-dimensional Mott states of spin-one bosons can be found in [6].
[19] A.F. Andreev and I.A. Grischuk, *Zh. Exp. Teor. Fiz.* **87**, 467 (1984)[*Sov. Phys. JETP* **60**(2), 267 (1984)].
[20] A.V. Chubukov, *J. Phys. Cond. Mat.* **2**, 1593 (1990); *Phys. Rev. B* **43**, 3337 (1991).
[21] P. Chandra, P. Coleman and A. I. Larkin, *J. Phys. Cond. Mat.* **2**, 7933 (1990).